PNAS RESEARCH ARTICLE | DEVELOPMENTAL BIOLOGY OPEN ACCESS

Mammalian life depends on two distinct pathways of DNA damage tolerance

Olimpia Alessandra Buoninfante[a,1], Bas Pilzecker[a,1], Aldo Spanjaard[a,1], Daniël de Groot[a,1], Stefan Prekovic[b,c], Ji-Ying Song[d], Cor Lieftink[e], Matilda Ayidah[a], Colin E. J. Pritchard[f], Judith Vivié[g], Kathleen E. Mcgrath[h], Ivo J. Huijbers[f], Sjaak Philipsen[i], Marieke von Lindern[j], Wilbert Zwart[b], Roderick L. Beijersbergen[e], James Palis[h], Paul C. M. van den Berk[a], and Heinz Jacobs[a,2]

Edited by Tasuku Honjo, Kyoto Daigaku, Kyoto, Japan; received September 20, 2022; accepted November 29, 2022

DNA damage threatens genomic integrity and instigates stem cell failure. To bypass genotoxic lesions during replication, cells employ DNA damage tolerance (DDT), which is regulated via PCNA ubiquitination and REV1. DDT is conserved in all domains of life, yet its relevance in mammals remains unclear. Here, we show that inactivation of both PCNA-ubiquitination and REV1 results in embryonic and adult lethality, and the accumulation of DNA damage in hematopoietic stem and progenitor cells (HSPCs) that ultimately resulted in their depletion. Our results reveal the crucial relevance of DDT in the maintenance of stem cell compartments and mammalian life in unperturbed conditions.

DNA damage tolerance (DDT) | DNA damage response (DDR) | hematopoietic stem cells | erythropoiesis | embryonic lethality

Significance

This report documents for the first time the essential and selective relevance of DNA damage tolerance (DDT) in warranting the survival of HSPCs and mammalian life. DDT prevents the accumulation of DNA damage in HSPCs, which results in cell cycle defects and apoptosis. Defects in DDT promote the survival of cells expressing erythroid transcription factors KLF1. These insights indicate a novel molecular mechanism that regulates hematopoietic output in response to DNA damage.

Faithful duplication and transmission of genetic information is essential for life. During S-phase, DNA damage poses a unique challenge, because it can stall ongoing replication and promote the generation of toxic secondary lesions like DNA double-strand breaks. To prevent these deleterious effects, cells employ diverse DDT pathways that warrant continuation of replication and replisome stability in the presence of fork-stalling lesions. Four principal modes of DNA damage tolerance (DDT) have been identified: translesion synthesis (TLS), template switching, fork reversal, and repriming (1–5). In eukaryotes, TLS is the prominent DDT pathway (6), and it depends on highly specialized error-prone TLS polymerases that are activated by damage-inducible mono-ubiquitination of the DNA-clamp Proliferating Cell Nuclear Antigen (PCNA) at lysine residue 164 (PCNA-Ub). Independent of PCNA-Ub, Reversionless 1 (REV1) can recruit other Y-family members TLS polymerases via its C-terminal domain to promote TLS (1, 7, 8). Alternatively, PCNA-Ub can be further modified by K63-linked poly-ubiquitin chains, which facilitates DDT by template switching and fork reversal, which are relatively error-free, as these pathways avoid damage by using the intact, newly synthesized strand of the sister chromatid as template (4, 9, 10). Apart from its role in fork progression where lesions are tolerated, DDT provides an essential intermediate step in interstrand crosslink (ICL) repair (11).

Repair of genetic lesions is especially crucial for stem cells, which warrant tissue homeostasis and regeneration throughout the lifetime of an organism (12). Residence of stem cells in protective niches, as well as their dormancy in unperturbed conditions promote stem cell maintenance (13, 14). Additionally, the enhanced DNA repair machinery in stem cells compared to differentiated cells endow stem cells with a unique capability to preserve the genome in the context of genotoxic stress (15). Simultaneously, stem cells are prone to undergo apoptosis or differentiation when DNA damage persists (16). Indeed, defects in DNA repair impair stem cell fitness and can result in premature aging, anemia, cancer, and developmental defects (16–19).

Evolutionary, DDT components are highly conserved and are present in both prokaryotes and eukaryotes (20). While it is known that the absence of DDT results in hypersensitivity to DNA damage in many in vitro systems (21, 22), the role of DDT for mammalian development and health remains unclear. Here we demonstrate in mice, that a homozygous *Pcna*$^{K164R/K164R}$;*Rev1*$^{-/-}$ compound mutation is embryonic lethal. The absence of DDT results in the accumulation of DNA damage that depletes hematopoietic stem and progenitor cells (HSPCs), resulting in aberrant erythropoiesis and a severe anemia. The severe anemia in double-mutant (DM) embryos was associated with a survival advantage of erythroid-like cells within the Lineage^{-}/Sca1^{+}/cKit^{+} (LSK) compartment, which in DM embryos consisted partially of lymphoid-primed multipotent progenitor 4 cells (MPP4s). This erythroid-like cluster was dependent on erythroid transcription factor (TF) Krueppel-Like Factor 1 (KLF1). Our results demonstrate that DDT is essential for mammalian life and stem cell maintenance and implicate that erythroid TF KLF1 promotes

Author contributions: O.A.B., B.P., A.S., D.d.G., S.P., C.E.J.P., P.C.M.v.d.B., and H.J. designed research; O.A.B., B.P., A.S., D.d.G., S.P., J.-Y.S., C.L., M.A., J.V., K.E.M., J.P., and P.C.M.v.d.B. performed research; C.E.J.P., I.J.H., S.P., W.Z., and R.L.B. contributed new reagents/analytic tools; O.A.B., B.P., A.S., D.d.G., S.P., J.-Y.S., C.L., M.A., J.V., K.E.M., J.P., and P.C.M.v.d.B. analyzed data; M.v.L. and J.P. provided expert advice on hematopoiesis; W.Z. provided expert advice on ChIP; R.L.B. provided expert advice on screening; and O.A.B., B.P., A.S., M.v.L., and H.J. wrote the paper.

The authors declare no competing interest.

This article is a PNAS Direct Submission.

[1]O.A.B., B.P., A.S., and D.d.G. contributed equally to this work.

[2]To whom correspondence may be addressed. Email: h.jacobs@nki.nl.

This article contains supporting information online at https://www.pnas.org/lookup/suppl/doi:10.1073/pnas.2216055120/-/DCSupplemental.

Published January 20, 2023.

survival of the erythroid lineage in the context of DNA damage to warrant tissue oxygenation. These insights highlight the relevance of an intact DNA damage response (DDR) system to preserve HSPCs in non-diseased and pathological conditions.

Results

DDT Deficiency Is Embryonic Lethal and Compromises the HSPC Compartment. To study the requirement of DDT, we made use of mice with a K164R mutation in the *Pcna* gene at lysine 164 ($Pcna^{KR}$ or $Pcna^{K164R}$) mice, in which PCNA-Ubiquitin-dependent DDT is abolished (16, 23). Additionally, we established $Rev1^{-/-}$ mice carrying a large deletion of *Rev1* (*SI Appendix*, Fig. S1 *A* and *B*). Intercrosses of $Pcna^{WT/K164R}$;$Rev1^{+/-}$ mice did not result in viable $Pcna^{K164R/K164R}$;$Rev1^{-/-}$ homozygous DMs, whereas homozygous single mutants (SMs; either homozygous for $Pcna^{K164R}$ or for $Rev1^{-}$) were born at the expected Mendelian frequency (Fig. 1 *A* and *B* and *SI Appendix*, Fig. S1*C*). Loss of DM embryos occurred early during development, as we observed few DM embryos at day 14.5 (*SI Appendix*, Fig. S1*C*). DM embryos were considerably smaller than wild type (WT) or SM embryos (Fig. 1*C*), indicating that DDT is essential for growth and normal development during embryogenesis. The sparsity with which DM embryos were obtained at E18.5 from crossings of $Pcna^{WT/K164R}$; $Rev1^{+/-}$ embryos, necessitated crossings of $Pcna^{WT/K164R}$; $Rev1^{-/-}$ mice to increase the frequency of DM embryos. To speed up the analysis to some extent, we additionally analyzed embryos at E14.5. Both E14.5 and E18.5 embryos were used in this study as indicated.

The absence of DDT and the deficiency to repair DNA ICLs, particularly affects hematopoiesis (11, 16). Therefore, we examined the bone marrow (BM) at E18.5 and fetal liver (FL) of E18.5 DM embryos in more detail (Fig. 1 *D*–*H*). BM was nearly devoid of hematopoietic cells (Fig. 1*D*). In E18.5 DM FL, the LSK compartment of HSPCs was nearly ablated (Fig. 1 *F*–*H*), indicating a critical role of DDT to maintain HSPCs. These results reveal an essential role of DDT for mammalian viability, predominantly affecting hematopoiesis.

DDT Deficiency Increases Expression of DNA Damage Markers, Cell Cycle Checkpoints, and Apoptosis Pathways. To investigate how DDT deficiency affected the LSK compartment of DM and SM embryos, we applied SORT-Seq, with which cells are sorted with Fluorecence-Activated Cell Sorting (FACS) into distinct wells for scRNA-Seq, allowing us to match the single-cell transcriptomes with their identity as defined by flow cytometry (24) (Fig. 2*A*). E14.5 FL LSKs were sorted and labeled with the additional markers to discern long-term Hematopoietic Stem Cells (LT-HSCs) ($CD135^{-}/CD48^{-}/CD150^{+}$), short-term HSCs (ST-HSCs) ($CD135^{-}/CD48^{-}/CD150^{-}$), and multipotent progenitors (MPP) that differentiate into megakaryocyte/erythrocyte and myeloid progenitors (MPP2, $CD135^{-}/CD48^{+}/CD150^{+}$; MMP3, $CD135^{-}/CD48^{+}/CD150^{-}$) or common lymphoid progenitors (CLPs) (MPP4, $CD135^{+}/CD150^{-}$). First we analyzed the combined transcriptome data of all LSK cells. Consistent with a significant ablation of the LSK compartment, ingenuity pathway analysis (IPA) revealed substantially increased signaling in pathways related to DNA damage repair, cell cycle regulation, and apoptosis in DM LSK cells, and to a lesser extent, in SM LSK cells (Fig. 2*B*).

Cell cycle alterations were also observed with flow cytometry in LSK and myeloid subsets [common myeloid progenitor (CMP), granulocyte-macrophage progenitor (GMP), and megakaryocyte/erythrocyte progenitor (MEP) (25)]. Indeed, in E18.5 FL cells of $Rev1^{-/-}$ embryos, and for MEPs, also in DM embryos, where less of the cells were in S/G2-phase (Fig. 2*C*). However, we did not detect differences in cell cycle between LSKs from WT and DM mice, perhaps because the few remaining LSKs were forced out of quiescence to promote blood production. This is different from the single-cell RNA-sequencing data from E14.5 MPPs, which likely relates to the advanced hematopoietic crisis at E18.5. Replication stress and DNA damage compromise HSC functioning (26). To directly assess the level of replication stress responses and increased DNA damage, we examined levels of phosphorylated histone variant H2AX at S139 (γH2AX) (27) in LSKs, MEP, CMP, and GMP (Fig. 2*D*). Remarkably, compared to the near absence of LSK cells staining positive for γH2AX in the WT condition, about 10% stained positive in both SM FLs in the G1 phase, and 60% in the DM (Fig. 2*D*), suggesting that not only stalled replication forks require DDT, but perhaps also lesions in other cell cycles (28–31). A similar phenotype was observed for the subsequent oligopotent progenitors. In S/G2, about 50% of DM LSKs and oligopotent progenitors stained positive for γH2AX, whereas for $Pcna^{K164R}$embryos, the frequency of γH2AX-positive cells did not increase much, arguing that during replication, REV1, though not PCNA-ubiquitination, is required to prevent replication stress and DNA damage.

Notably, $Rev1^{-/-}$ embryos frequently had higher absolute numbers of hematopoietic cells than their WT counterparts (Fig. 1*H*, and most other figures in this manuscript), and those cells contained elevated levels of γH2AX (Fig. 2*D*). However, $Rev1^{-/-}$ animals featured no anemia (see figures below). We therefore hypothesize that the increased pool of hematopoietic precursor cells in $Rev1^{-/-}$ embryos minimizes cell cycle entry (Fig. 2*C*), thereby limiting the deleterious effects of replication stress. However, the percentage of γH2AX-positive cells significantly increased in double-mutant embryos compared to $Rev1^{-/-}$ embryos, indicating that PCNA-ubiquitination can partially compensate for the effects on replication stress imposed by deficiency of REV1. Importantly, the majority of stem and progenitor cells of double-mutant embryos contained increased frequencies of γH2AX-positive cells; these results indicate the absolute requirement of the DDT system to prevent DNA damage and replication stress in the hematopoietic system. We hypothesize that the increased level of cycling hematopoietic cells of DM embryos (Fig. 2*C*) compared to $Rev1^{-/-}$ embryos is a compensatory mechanism of the hematopoietic system to maintain hematopoietic output.

Erythroid Lineage Cells Are Maintained in the LSK and Myeloid Compartment in Absence of DDT. To examine how DDT deficiencies altered HSPC makeup at the single-cell level, we analyzed SORT-Seq data, this time at the single-cell level. As expected, LT-HSCs were less present in DM embryos, whereas erythroid-primed MPP2s appeared increased (Fig. 3*A*). Uniform Manifold Approximation and Projection (UMAP) clustering of single-cell transcriptomes revealed the existence of three clusters that were populated by all cell types (Fig. 3*B* and *SI Appendix*, Fig. S2*A*). One cluster, from here on termed cluster 2, was separated from the main cluster—cluster 1—in all embryos, and importantly was maintained in DM embryos (Fig. 3 *B* and *C*).

Analyses of cluster 2 revealed high expression of erythroid lineage-associated TFs such as *Klf1*, *Zbtb7a,* and *Gata1* (32–34), compared to all other cells, as indicated by the positive Z-score (Fig. 3*D*), which strongly suggested that these cells were erythroid-biased. The erythroid signaling in this cluster was moreover substantiated by high expression of the Erythropoetin (EPO) receptor, *Epor* (Fig. 3*D*). Gene Ontology (GO) analysis revealed that cluster 2, compared to clusters 1 and 3, featured a higher

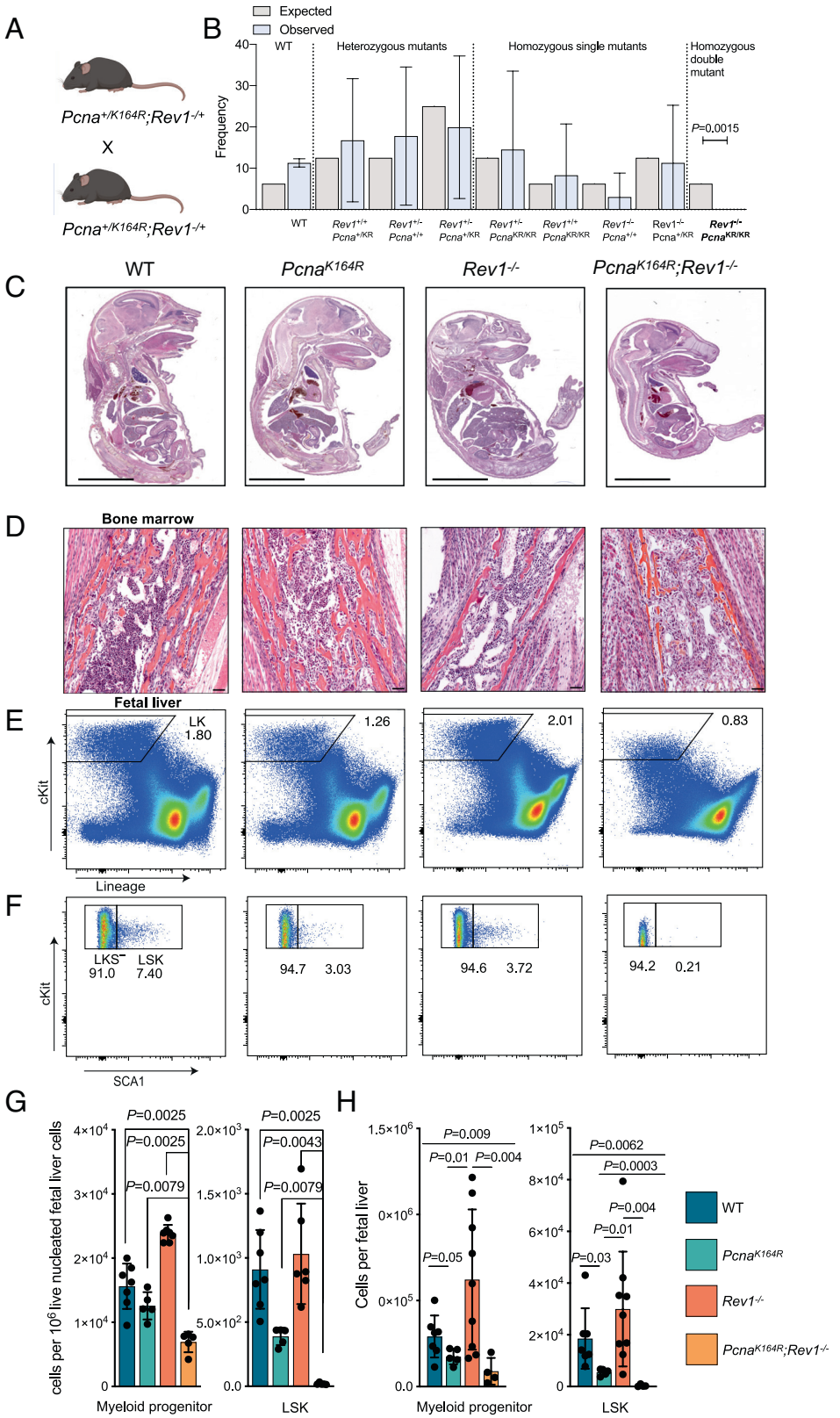

Fig. 1. Absence of DDT results in embryonic lethality and severe hematopoietic stem cell failure. *A*, Breeding scheme to obtain DM embryos and mice. *B*, Observed and expected frequencies of offspring, obtained from $Pcna^{K164R/+}Rev1^{+/-}$ intercrosses (Fisher's exact test, 95% CI, n = 166, from 26 breeding pairs). *C*, Representative sagittal sections of WT, SMs, and $Pcna^{KR}$ $Rev1^{-/-}$ genotypes at E18.5. (Scale bar, 5 mm.) *D*, Microphotographs of H&E sections of BM from WT and $Pcna^{K164R}$ $Rev1^{-/-}$ E18.5. The $Pcna^{K164R}$ $Rev1^{-/-}$ BM showed the absence of hematopoietic cells which were replaced by stromal cells. Furthermore, the controls did show the presence of numerous dark-blue myeloid cells. (Scale bars, 50 µm.) *E* and *F*, Gating strategy and representative frequencies of $Lin^{-}cKit^{+}$ cells, myeloid progenitors (LKS^{-}) and LSK of FL from WT and $Pcna^{K164R}$ $Rev1^{-/-}$ E18.5 embryos. *G* and *H*, Relative (*G*) and absolute (*H*) numbers of the defined hematopoietic subsets in *E* and *F*. In each graph, the bar represents the mean ± SD. WT n = 7, $Pcna^{K164R}$ n= 5, $Rev1^{-/-}$ n = 6, $Pcna^{K164R}$ $Rev1^{-/-}$ n= 5. Same in *G* and *H* but in *H*, the n for $Rev1^{-/-}$ is 9. The graphs indicate specific cells counts per 10^{-6} of live FL cells. *P* values were calculated using unpaired *t* test with Welch's correction.

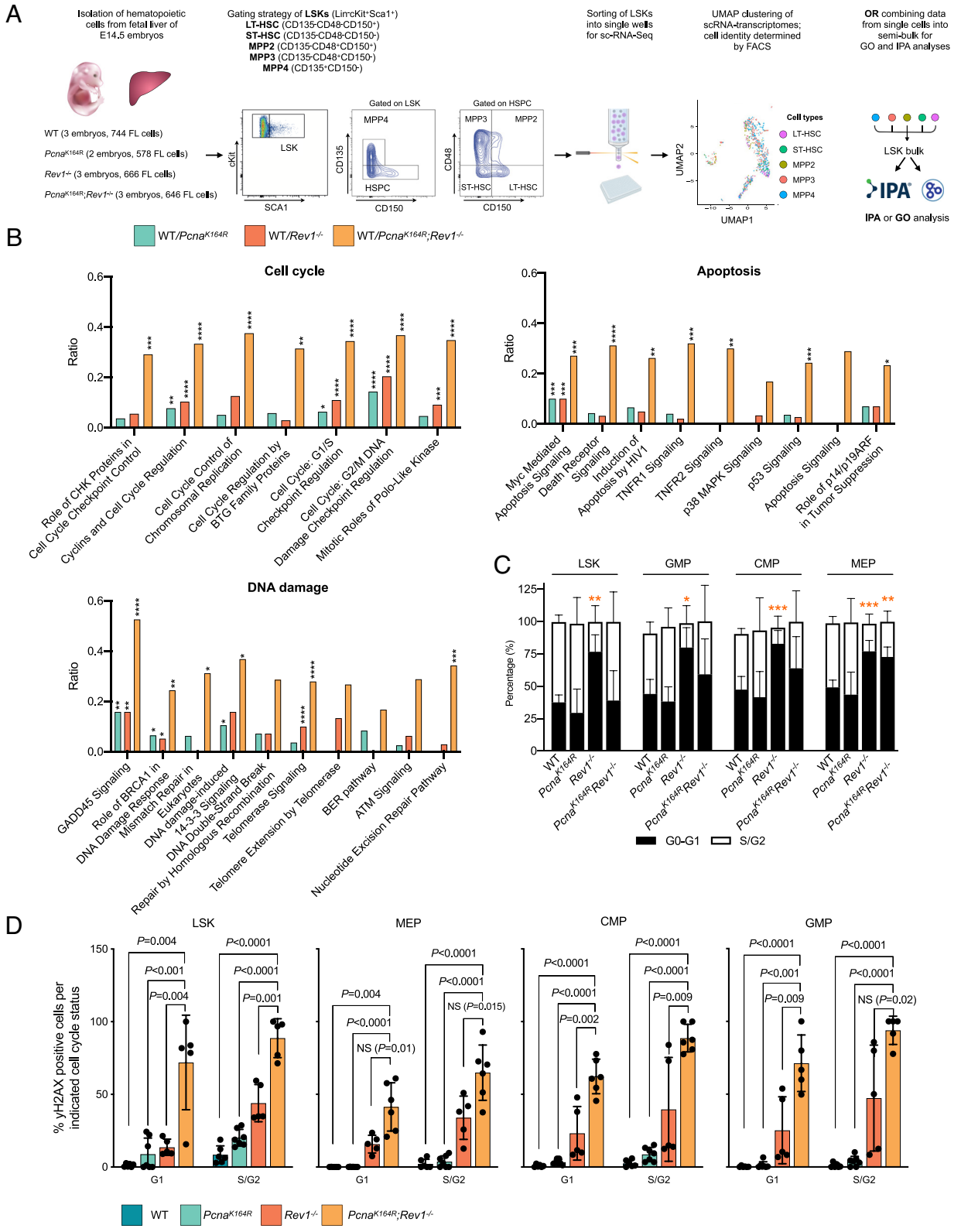

Fig. 2. DDT deficiency results in DNA damage, apoptosis and cell cycle checkpoint activation in HSPCs. *A*, Analysis of transcriptomes by the SORT-Seq approach: FLs were isolated from E14.5 embryos, and LT-HSC, ST-HSC, and MPP2-4 cells from the LSK compartment were sorted into single wells, followed by scRNA-seq, allowing for downstream matching of the transcriptome with each cell type. For some analyses in this figure, transcriptomes from single cells were pooled into a semi-bulk, allowing for IPA analysis. *B*, Histogram representing the ratio between the number of DE genes associated with the cell cycle divided by total number of genes in cell cycle genes, enriched in each mutant compared to the WT as identified by IPA. The analysis for other graphs was the same, but here, the IPA identified DNA damage pathways, and senescence and cell death pathways were used. *P* values calculated using a right-tailed Fisher's exact test with a Benjamini–Hochberg correction for multiple testing. *C*, Cell cycle state as analyzed by DAPI staining in LSK and myeloid progenitor cells from E18.5 FLs. *P* values calculated using unpaired *t* test with Welch's correction. *D*, Percentage of γH2AX positive HSPCs in G1 and S/G2 of the cell cycle. The columns represent the mean ± SD. WT n = 6, *Pcna*^{K164R} n= 7, *Rev1*$^{-/-}$ n = 5, *Pcna*^{K164R} *Rev1*$^{-/-}$ n= 5. *P* values calculated using unpaired *t* test with Welch's correction.

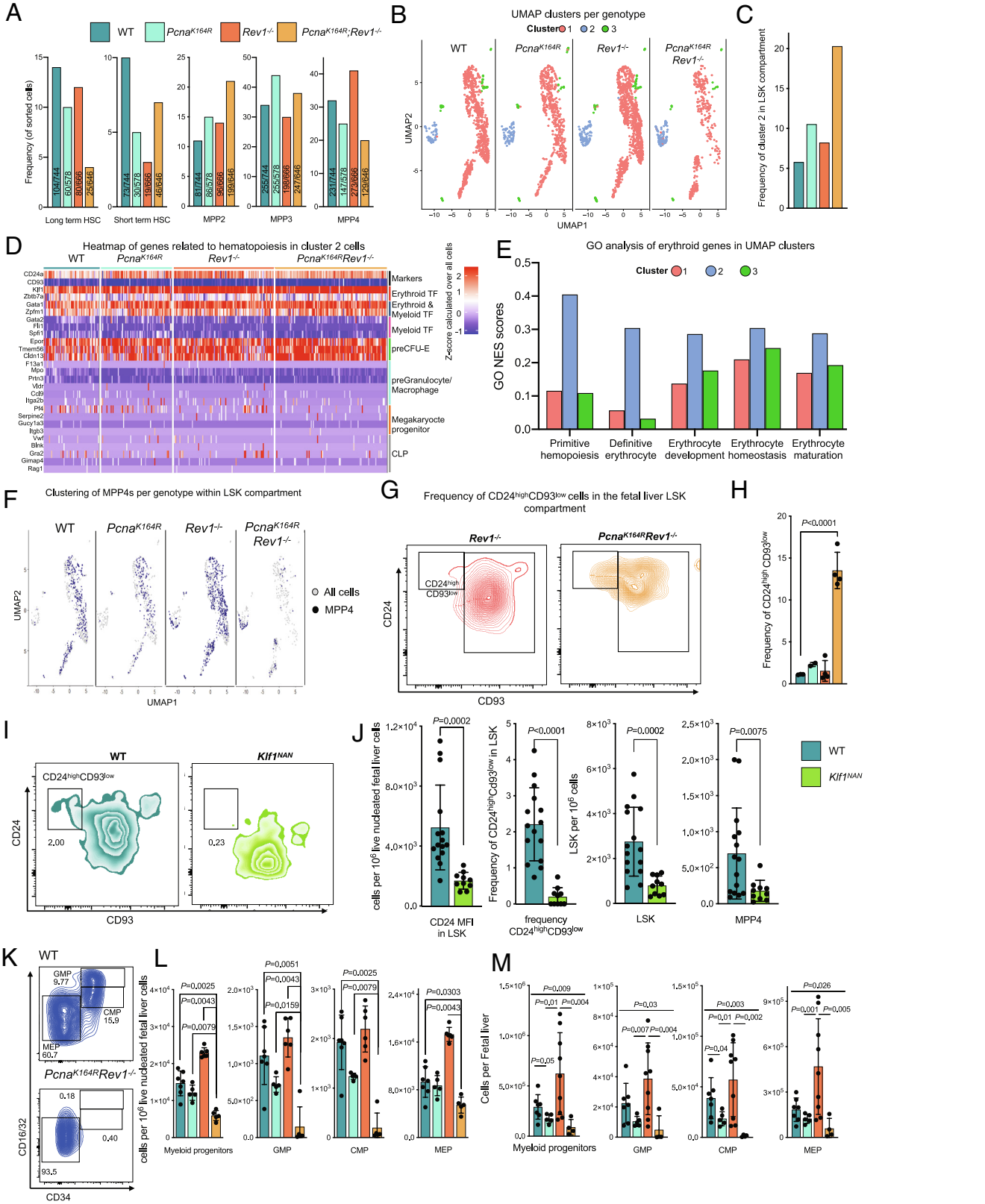

Fig. 3. Erythroid cells present in LSKs and myeloid progenitors selectively remain in DM embryos. *A*, Percentages and numbers of indicated cell subsets sorted for SORT-Seq within the E14.5 LSK compartment. *B*, Single-cell transcriptome-based UMAP clustering of indicated genotypes. Color-coded cells correspond to indicated clusters. *C*, Quantification of the frequency of cells belonging to cluster 2 in each genotype, as determined by the SEURAT algorithm. *D*, Heatmap of handpicked genes related to differentiation of MEPs, CLPs, GMPs as well as depiction of marker genes of cluster 2 per genotype. *E*, GO analysis of differential genes of cluster 2 compared to the clusters, error bars denote GO scores of clusters from all embryos combined (total n = 11). *F*, Residence of MPP4s in each cluster, shown as the UMAP plots of SORT-Seq. Note the increased residence of MPP4s in cluster 2 in Rev1-/- and DM embryos. *G*, FACS representative example of $CD24^{high}$ $CD93^{low}$ population in $Rev1^{-/-}$ and DM FL LSKs. *H*, Frequency of $CD24^{high}$ $CD93^{low}$ population by flow cytometry in FL LSKs. *I*, FACS gating of LSKs, containing $CD24a^{high}CD93^{low}$ subset in WT and $Klf1^{NAN}$ E18.5 embryos. *J*, In each graph, the bar represents the mean ± SD. WT n = 15, $Klf1^{NAN}$ = 10. Quantification of CD24 MFI of LSK cells (*Left*) and frequency of $CD24a^{high}CD93^{low}$ population in WT and NAN E18.5 (*Middle*). The graphs on the right indicate specific cells counts per 1×10^{-6} of live cells. *P* values were calculated using unpaired *t* test with Welch correction. *K*, Composition of the myeloid compartment in WT and DM embryos. *L* and *M*, Relative (*L*) and absolute (*M*) numbers of indicated myeloid compartment cells. In each graph, the bar represents the mean ± SD. n for *L*: WT n = 7, $Pcna^{K164R}$ n= 5, $Rev1^{-/-}$ n = 6, $Pcna^{K164R}$ $Rev1^{-/-}$ n= 5. n for *M*: WT n = 7, $Pcna^{K164R}$ n= 5, $Rev1^{-/-}$ n = 9, $Pcna^{K164R}$ $Rev1^{-/-}$ n= 4. *P* values were calculated using unpaired *t* test with Welch's correction.

score for pathways related to erythropoiesis (Fig. 3*E*). TFs required for differentiation into megakaryocytes, platelets, granulocytes, and macrophages were nearly undetectable (Fig. 3*D*), whereas all cells of cluster 2 expressed erythroid-specific TFs, suggesting that cells from cluster 2 became erythroid-biased. The expression levels of erythroid TFs remained relatively constant between genotypes, which implies that increased frequency of cluster 2 cells compared to other cells in DM embryos does not depend on expression level of erythroid TFs, but rather that cells from cluster 2 remain intact in the absence of DDT, possibly due to a survival advantage compared to cells in the other clusters (see below).

Prior observations in mice have shown that in the context of hematopoietic stress, lymphoid-primed MPP4s become transcriptionally similar to erythroid and myeloid-primed MPP2/3 cells (35). We therefore speculated that cells in cluster 2 in DM embryos would consist partially of MPP4s. The analysis of cluster 2 in WT and SM embryos revealed that it predominantly comprised of erythroid and myeloid-primed MPP2s and MPP3s (*SI Appendix*, Fig. S2*B*). Strikingly, in DM embryos, and to some extent in *Rev1*$^{-/-}$ embryos, CLP-primed MPP4s were detected in cluster 2 (*SI Appendix*, Fig. S2*B*). In contrast to WT and SM embryos, in DM embryos, MPP4s were rarely detected in cluster 1 (Fig. 3*F*). CLP TFs were not expressed in cluster 2 (Fig. 3*D*), indicating that under stress-induced conditions in *Rev1*$^{-/-}$ and DM embryos, CLP-primed MPP4s can redirect their normal transcriptome in response to DNA damage toward erythroid-primed MPP2s and MPP3s. These results revealed that MPP4s are plastic, as reported previously, and can be skewed toward cluster 2 cells. Furthermore, these data indicate that hematopoietic skewing is at least partially responsible for the maintenance of cluster 2. These results are consistent with earlier observations (35), and highlight an intricate connection between lymphoid-primed and erythroid-primed cells in compensating the hematopoietic stress conditions imposed by DNA damage.

To validate the dependency of cluster 2 cells on erythroid TFs, we first determined if these cells could be identified using flow cytometry. We examined expression of potential surface markers in the transcriptome data and identified *Cd24a*—which has been shown to be expressed by early erythroid cells during embryogenesis (36, 37)—and *Cd93,* which were up- and downregulated, respectively (Fig. 3*D*). Importantly, using flow cytometry, we could identify a CD24a^{high}CD93^{low} cluster in LSKs at E18.5, which increased in frequency in DM embryos (Fig. 3 *G* and *H*). As key erythroid TF *Klf1* was uniformly highly expressed in cluster 2 cells, we examined cluster 2 cells were dependent on its expression. Here, we took advantage of the dominant negative *Klf1* (*Klf1*^{Nan}) mutant embryos (38) at E18.5. *Klf1*^{Nan}homozygous mutant mice die during early embryogenesis, while heterozygous mice develop hemolytic anemia in embryonic and adult stages (39). Using CD24A and CD93 as markers for cluster 2, we analyzed the LSK compartment in E18.5 FLs from heterozygous dominant-negative *Klf1*^{Nan}embryos. We observed a significant reduction of cluster 2, expression of CD24 in this cluster, and a reduction in LSKs and MPP4s in the mutant embryos (Fig. 3 *I* and *J*), indicating that the essential erythroid TF KLF1 is also crucial for cluster 2 cells.

While CMPs give rise to erythroid cells, erythroid lineage differentiation likely originates within the MPP compartment (40). We therefore speculated that the selective maintenance of erythroid-like cluster 2 in DM embryos would result in increased erythroid commitment in the CMPs. We assessed myeloid progenitors, which ultimately differentiate into erythroid-producing MEPs, or granulocyte-macrophage progenitors (GMPs). Consistent with the selective maintenance of erythroid-lineage cells, remaining progenitors in DM embryos were predominantly MEPs (Fig. 3 *K–M*), indicating erythroid-forming progenitors selectively remain in DM embryos, likely to counteract anemia and promote tissue oxygenation. At the moment, we cannot say whether the "intactness" of cluster 2 cells and MEPs is the result of skewed differentiation, reduced apoptosis, or both. Importantly, these results indicate that erythroid lineage cells prevail compared to non-erythroid cells in the context of DNA damage-induced attrition. Finally, consistent with altered differentiation of lymphoid-primed MPP4s in DM embryos, we noted a near-significant block in thymocyte differentiation (*SI Appendix*, Fig. S3 *A–E*) and a severe block in B cell development (*SI Appendix*, Fig. S3 *F–H*) in DM embryos.

DDT-Deficient Mice Feature Multiple Hallmarks of Anemia. The strong absence of LSKs and the relative intactness of HSPCs and myeloid progenitors that ultimately can become erythroid cells suggested that in absence of DDT, erythroid output was favored, likely to counteract anemia resulting from reduced numbers of HSPCs and myeloid progenitors. However, this clearly was not enough to prevent embryonic lethality in DM embryos, suggesting that erythrocyte production was compromised. To determine whether erythrocyte maturation was affected in DM embryos, we examined the maturation of erythroid precursors in the DM E18.5 whole FL by flow cytometry. We observed that early erythroid precursors, such as ProE and EryA, were increased in DM embryos, whereas later-stage EryB and EryC precursors were decreased (Fig. 4 *A–C*). Moreover, red blood cells, both in the FL and in the blood, were severely decreased in DM embryos (Fig. 4*D*). These results suggest that erythrocyte maturation is affected most at the EryC and downstream stages. The analysis of hemoglobin levels revealed that while overall levels of hemoglobin were significantly decreased in DM embryos, its expression on a per corpuscle basis was markedly increased, consistent with anemia (Fig. 4*D*).

The flow cytometry data suggested that erythroid output in FLs was compromised. To examine whether this resulted in hallmarks of stressed erythropoiesis, we examined blood films at E18.5, and observed characteristics of abnormal erythrocyte maturation (Fig. 4 *E* and *F*), such as polychromasia and anisocytosis, nucleated red blood cells, and basophilic inclusion bodies (Fig. 4*F*). Howell-Jolly bodies can be observed in DNA damage disorders and are indicative of halted DNA synthesis or repair (41). These results indicate that DDT is required for proper erythrocyte development, and that its absence results in severe anemia.

DDT Is Required for Adult Hematopoiesis. Because embryonic development requires continuous cell division, and because murine adult HSCs are relatively quiescent (42), we examined the effect of DDT deficiency on adult mice. We previously reported that *Pcna*^{K164R}mice featured impaired hematopoiesis, which was reconfirmed in this study (Fig. 5*A*). In contrast, hematopoiesis was not affected in *Rev1*$^{-/-}$ adult mice. To assess the requirement of both DDT pathways in adult mice, we established a *Pcna*$^{K164R/K164\text{-}LoxP}$;*Rev1*$^{-/-}$;Confetti;*Rosa26*-Cre^{ERT2} mouse models where tamoxifen administration induced generation of DM cells, as well as expression of the confetti construct that allowed us to track deleted cells (Fig. 5 *B* and *C*). *Pcna*$^{K164/K164\text{-}LoxP}$;*Rev1*$^{-/+}$served as controls (Fig. 5*B*). Two weeks after tamoxifen administration, all analyzed hematopoietic compartments (Lin^{-}cKit^{+}, LSK, and myeloid progenitors) were ablated in DM but not WT mice (Fig. 5*D*). The percentage of Confetti-positive cells remained stable in control mice but significantly decreased in DM mice from 2 to 4 wk following tamoxifen treatment indicating a reduced capacity to replenish functional blood cells (Fig. 5*D*). These results reveal that DDT is required for adult hematopoiesis, and by extension, for mammalian life.

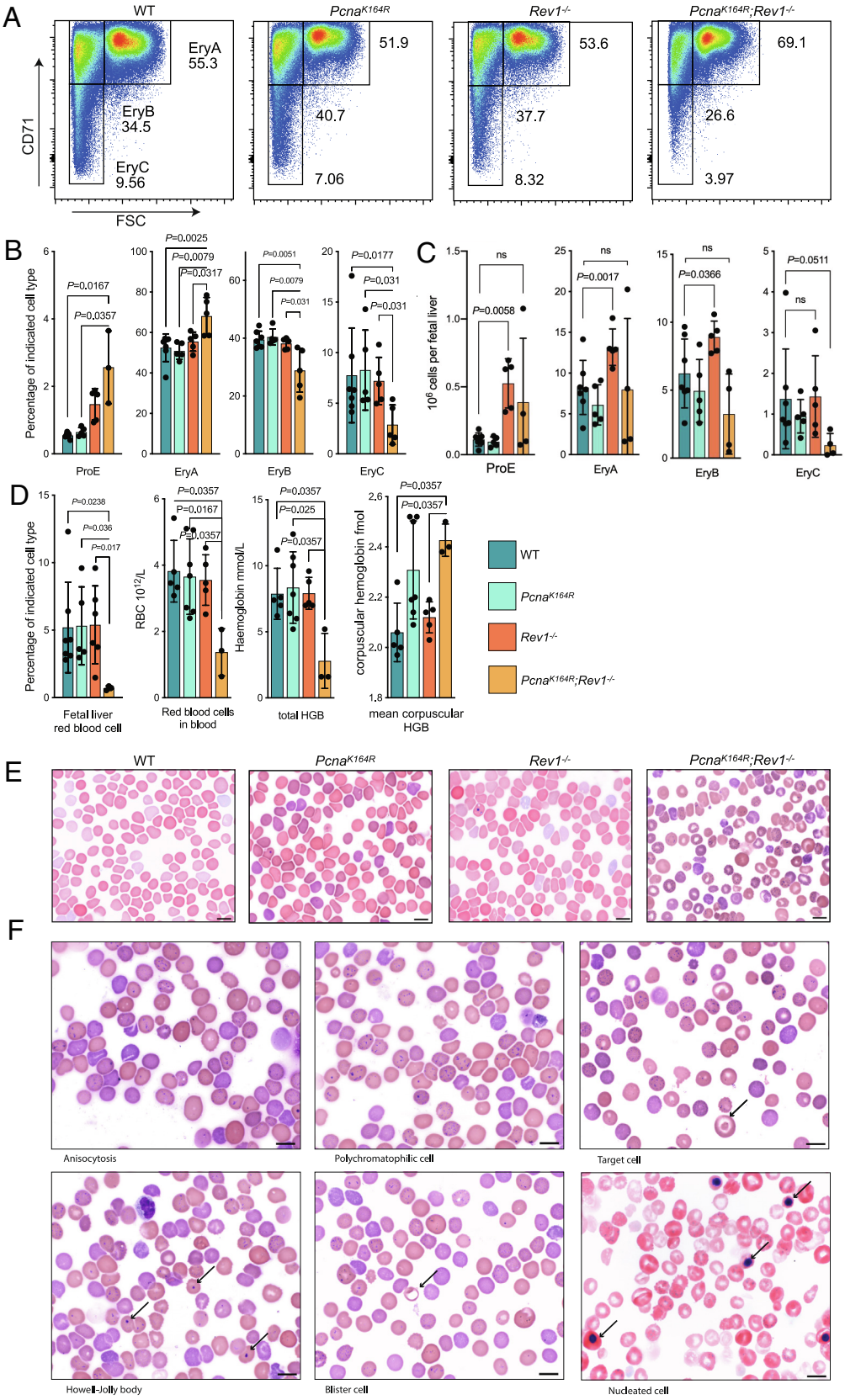

Fig. 4. DM embryos feature stressed erythropoeiesis and suffer from severe anemia. *A*, Gating strategy of EryA-C erythroid cells from E18.5 $Pcna^{K164R}$ $Rev1^{-/-}$ and control FLs. *B* and *C*, Blood cell maturation percentages (*B*) and absolute numbers (*C*) in FLs of $Pcna^{K164R}$ $Rev1^{-/-}$ embryos. Central line represents the mean ± SD. WT n = 7, $Pcna^{K164R}$ n= 5, $Rev1^{-/-}$ n = 5, $Pcna^{K164R}$ $Rev1^{-/-}$ n= 3. *P* values were calculated using Mann–Whitney *U* test. *D*, Frequency of erythrocytes in the FL, RBC count, and hemoglobin levels of RBCs. Central line represents the mean ± SD. WT n = 5, $Pcna^{K164R}$ n= 7, $Rev1^{-/-}$ n = 5, $Pcna^{K164R}$ $Rev1^{-/-}$ n= 3. *P* values were calculated using Mann–Whitney *U* test. *E*, Wright–Giemsa's blood films of DMs, SMs and controls. DMs show signs of severe anemia. (Scale bar, 10 μm.) *F*, Microphotographs examples of Wright–Giemsa's blood films of DM E18.5 embryos. Examples of anemic phenotype consist of: anisocytosis (variation in cell size: a mixed population of microcytes and macrocytes), polychromasia (reticulocytes), target cell (arrow), nucleated RBC (arrows), cells with basophilic inclusion body, blister cell (arrow), and Howell-Jolly bodies. (Scale bars, 10 mm.)

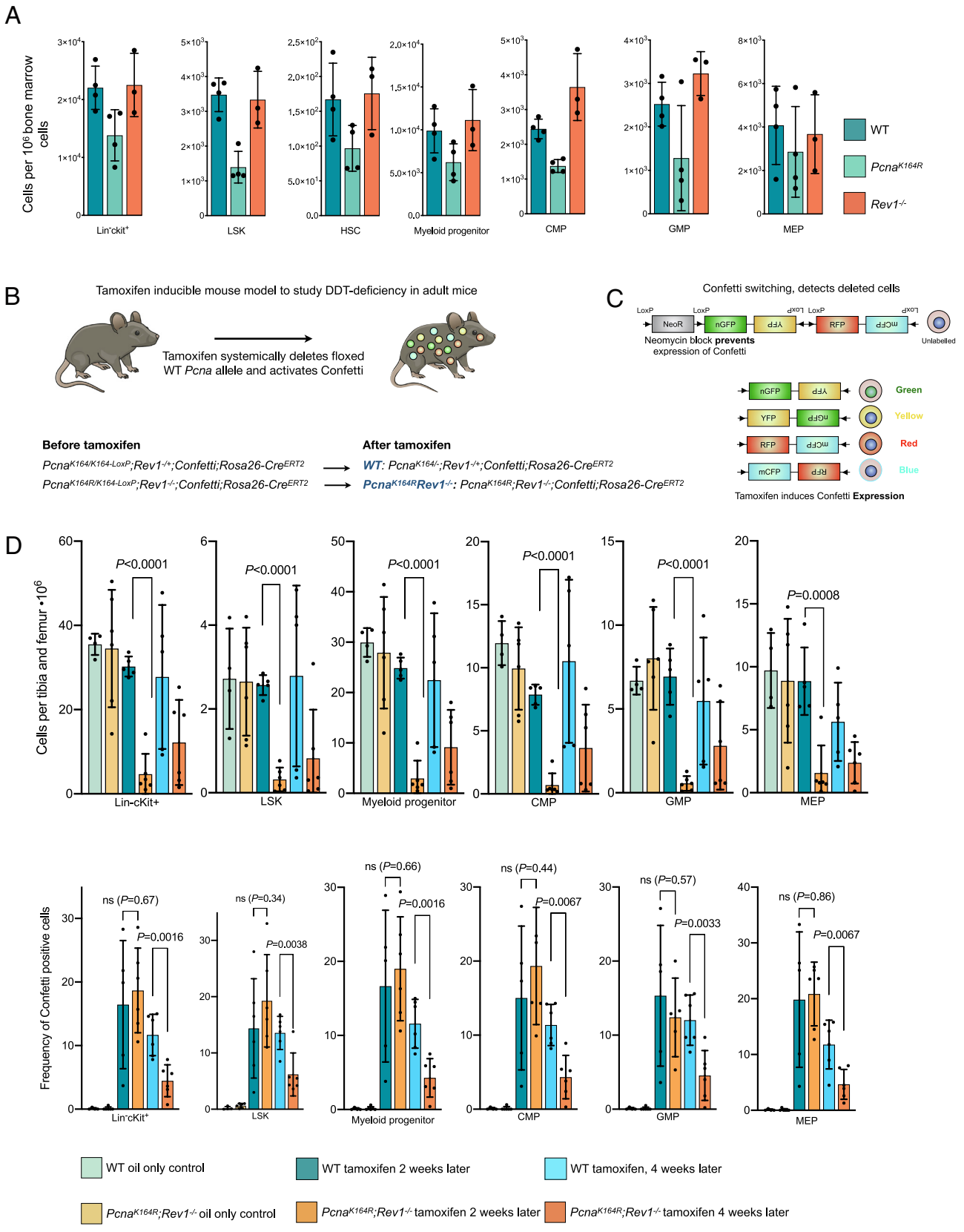

Fig. 5. Absence of PCNA ubiquitination and REV1 is lethal in adult mice. *A*, Relative number of indicated cells of indicated genotypes in the BM of adult mice SM mice. *B*, Inducible inactivation of DDT in adult mice: Conditional ablation of a floxed PCNA allele in mice that feature a non-floxed PCNA-K164 or K164R allele results in the generation of PCNA-ub-dependent DDT-deficient mice, and "WT" controls. In the absence of functional REV1, this tamoxifen-inducible deletion results in the generation of DM mice. WT controls feature a heterozygous deletion of *Rev1*. *C*, Activation of the Cre^{ERT2} in the mice by intraperitoneal injection of tamoxifen results in the genetic rearrangement of the confetti construct present in the mice. This allows for long-term tracing of deleted cells in mice by determining the frequencies of cells expressing GFP, RFP, YFP, or CFP. *D*, (*Top*) The graphs indicate specific cells counts per 1×10^{-6} of single cells, after twp tamoxifen injections (right part of the graph), or after oil injection (left part of the graph). Data were pooled from two independent experiments. (*Bottom*) The graphs indicate the percentage of confetti-positive cells (expressing one or more colors of the confetti construct), after two tamoxifen injections after 2 and 4 wk (middle and right part of the graph), or after oil injection (left part of the graph). Data were pooled from two independent experiments. *P* values were calculated using an unpaired *t* test. From left to right, n = 4, 6, 5, 6, 5, 6.

Discussion

DDT is regulated by PCNA-Ub and REV1. The introduction of a *Pcna*^{K164R}*Rev1*$^{-/-}$ DM compound mutation in the mouse germline was found lethal during embryogenesis and in a conditional model lethal in adult mice. These genetic approaches revealed a non-epistatic relation between PCNA ubiquitination and REV1-dependent DDT, and firmly establish their critical role as essential players within the DDR network.

Pathological analysis uncovered that compound mutant embryos suffered from severe anemia, which was associated with a severely diminished myeloid cell compartment. Furthermore, in-depth cellular and molecular analyses defined a critical role of DDT in ensuring long-term HSC survival and homeostasis in the blood system. In the absence of DDT, the LSK compartment featured increased DNA damage, and upregulated cell cycle and apoptotic pathways, which directly linked to HSC exhaustion. scRNA-Seq of the LSK compartment revealed that a KLF1-dependent cluster of cells expressing erythroid TFs and erythroid development pathways remained intact in DM embryos. Downstream of the LSK compartment, similar observations were made in myeloid progenitors, with erythroid/myeloid progenitors remaining preferentially intact,

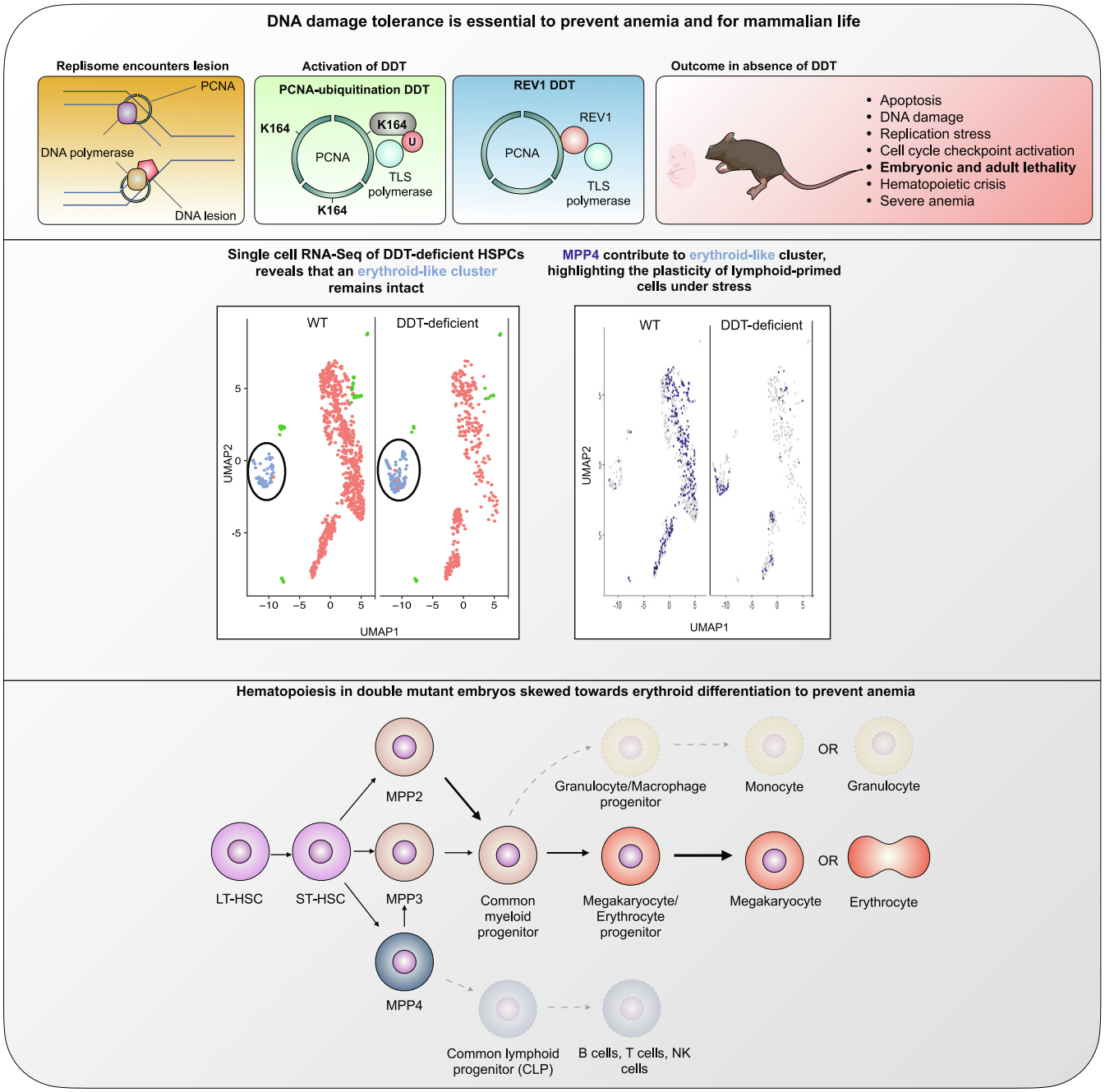

Fig. 6. Prolonging hematopoiesis in the absence of DDT: MPP4s support erythropoiesis. *Upper*: Inactivation of DDT through the inactivation of TLS recruitment by PCNA-Ub and REV1 causes replication stress, accumulation of DNA damage, cell checkpoint activation, and apoptosis in the hematopoietic system. Ultimately, these mutations lead to the development of lethal anemia in both, mouse embryos and adult mice. *Middle*: The hematopoietic crises caused by the lack of DDT reveals the persistence of an erythroid-like cluster, while other clusters are reduced. The persistence of this cluster appears to depend on the plasticity of MMP4, that are normally lymphoid committed. *Lower*: Proposed model of stressed hematopoiesis in DDT-deficient mice. Hematopoietic crises seen in double-mutant mice causes MPP4, normally committed to the lymphoid lineage cells, to differentiate toward erythroid-like progenitors. This plasticity ensures a prolonged erythroid output when canonical erythroid precursors are depleted as a consequence of genomic instability.

whereas non-erythroid progenitors were almost completely absent in DM embryos. Intriguingly, in *Pcna*^{K164R} and Rev1$^{-/-}$ mice, we observed a different cell cycle phenotype in the LSK and myeloid compartment. This difference likely relates to our previous findings, where compared to REV1, PCNA-Ub-dependent DDT was found involved in tolerating the vast majority of replication-blocking lesions (43). Accordingly, replication stress is expected to accumulate faster in the absence of PCNA-Ub-dependent DDT leading to cell death, whereas the absence of REV1 cells replication stress accumulates more slowly, favoring their arrest in G0 to G1.

In the LSK compartment, specifically in *Rev1*$^{-/-}$ and DM embryos, we identified a subcluster of the MPP4 cells that were transcriptionally similar to the cells in the erythroid-like cluster. This is quite remarkable considering that under steady-state conditions MPP4 are expected to give rise predominantly to lymphoid committed cells (44). Intriguingly, the skewing of MPP4s toward cluster 2 was also observed in *Rev1*$^{-/-}$ embryos, though not in *Pcna*^{K164R}embryos, and as neither of these embryos was anemic. These results suggest that replication stress is sufficient to directly drive skewing of MPP4s.

Despite the relative maintenance of erythroid progenitors, DM embryos died during development, and as stated before, live mice were never obtained. Clearly, the maintenance of erythroid progenitors did not prevent lethality, suggestive of anemia. Indeed, examination of the blood revealed several hallmarks of stressed hematopoiesis, and reduced maturation of erythroid cells. Howell-Jolly bodies—staining of DNA fragments—that were present in the erythroid cells indicated transmission of DNA damage to erythrocytes, potentially explaining their maturation defects.

The examination of non-hematopoietic tissues and organs did not reveal notable defects in DM embryos, nor did staining with DNA damage markers 53BP1 or γH2AX. Although DM embryos died early during development, and though they were smaller—indicating that non-hematopoietic cells are likely also affected, these results strongly suggest that both pathways of DDT are most critical to prevent collapse of the hematopoietic system. Similar observations were made in adult DM mice, where pathologies were not detected in organs other than the hematopoietic system. Hematopoiesis is primarily established during embryogenesis, and adult murine HSCs have been observed to cycle very infrequently. Our results indicate that DDT is essential for both actively cycling murine and quiescent HSCs.

Our work established that DDT is a critical contributor to the DDR network and warrants hematopoiesis and mammalian life. scRNA-Seq revealed an early KLF1-dependent erythroid compartment existed within the LSK compartment that preferentially remained intact in DM embryos, likely due to skewing of MPP4s to this compartment (Fig. 6). Within the myeloid compartment, selective survival of the MEP compartment was also observed, highlighting plasticity of the hematopoietic system in the context of DNA damage-induced stress. Mechanistically, our results suggest that skewing of hematopoiesis to counteract anemia depends on the activation of the important erythroid TF KLF1. In conclusion, here, we show for the first time the importance of DDT for mammalian life and in particular the fitness of HSPCs.

Materials and Methods

For detailed Materials and Method, see *SI Appendix*.

Mice and Cell Lines. Experiments were approved by an animal ethics committee of the Netherlands Cancer Institute (Amsterdam, Netherlands). *Pcna*^{K164R}mice have been described previously (16, 23). CRISPR/*Cas9* was used to generate a new *Rev1*$^{-/-}$ mouse strain (*SI Appendix*, Fig. S1*A*). Double-mutant embryos were obtained via intercrosses. Similar procedures were performed to generate Confetti;*Rosa26*-Cre^{ERT2}; *Pcna*$^{K164R/K164-F}$or *Pcna*$^{K164/K164-FL}$;*Rev1*$^{-/+}$or *Rev1*$^{-/-}$;Confetti mice. Tamoxifen conditionally ablated DDT in adult mice. Heterozygous *Klf1*^{Nan}males (38) were set up with WT C57BL/6 females.

Histopathological Analysis and Ex Vivo Immunophenotyping. Embryos were fixed in Ethanol Acetic acid Formaldehyde (EAF) stained with H&E for pathological analysis. Beckman Coulter counter (DxH500) was used to analyze blood composition. Blood smears were stained with Wright-Giemsa. FL cells were used for immunophenotyping studies. Antibodies were used to identify HSPCs on FLs and BM cells and to sort single cells from FLs. Similar procedures were performed to analyze the BM of adult DDT-deficient mice.

Single-Cell RNA Sequencing. SORT-Seq and mapping were performed as previously described (24) on FACS-sorted LSK cells. The downstream analysis was performed using Seurat in R. An IPA (Qiagen/version: 01-06) was used for pathway analysis, and IPA genes were used for pathway enrichment analysis.

Genotyping. To confirm genotypes of mice and cells, samples were lysed in lysis buffer containing ProtK followed by PCR (*SI Appendix*, Fig. S1).

Data, Materials, and Software Availability. Single cell RNA sequencing data were deposited in GEO under the accession number GSE122784.

ACKNOWLEDGMENTS. We like to thank N. Wit and F. Alemdehy for comments on the manuscript, members of the FACS facility for assistance during sorting and flow cytometric analysis, the biotechnical staff of the Netherlands Cancer Institute - Antoni van Leeuwenhoek Mouse Clinic for Cancer and Aging (MCCA) for biotechnical support, C. Göbel for help with ChIP-Seq experiments, and all the members of mouse facility for assistance in maintenance of mice. Portions of this work were developed from the doctoral dissertation of O.A.B.

Author affiliations: [a]Division of Tumor Biology and Immunology, The Netherlands Cancer Institute, 1066CX Amsterdam, The Netherlands; [b]Division of Oncogenomics, The Netherlands Cancer Institute, 1066CX Amsterdam, The Netherlands; [c]Center for Molecular Medicine, University Medical Center Utrecht and Utrecht University, 3584 CX Utrecht, The Netherlands; [d]Division of Experimental Animal Pathology, The Netherlands Cancer Institute, 1066CX Amsterdam, The Netherlands; [e]Division of Molecular Carcinogenesis, The Netherlands Cancer Institute Robotics and Screening Center, The Netherlands Cancer Institute, 1066CX Amsterdam, The Netherlands; [f]Mouse Clinic for Cancer and Aging Research, Transgenic Facility, The Netherlands Cancer Institute, 1066 CX Amsterdam, The Netherlands; [g]Hubrecht Institute-Royal Netherlands Academy of Arts and Sciences, 3584 CT Utrecht, The Netherlands; [h]Department of Pediatrics, University of Rochester Medical Center School of Medicine and Dentistry, Rochester, NY 14642; [i]Department of Cell Biology, Erasmus Medical Center, 3015CN Rotterdam, The Netherlands; and [j]Department of Hematopoiesis, Sanquin Research and Landsteiner Laboratories, 1066CX Amsterdam, The Netherlands

1. G. L. Moldovan, B. Pfander, S. Jentsch, PCNA, the maestro of the replication fork. *Cell* **129**, 665–679 (2007).
2. E. C. Friedberg, Suffering in silence: The tolerance of DNA damage. *Nat. Rev. Mol. Cell Biol.* **6**, 943–953 (2005).
3. J. E. Sale, A. R. Lehmann, R. Woodgate, Y-family DNA polymerases and their role in tolerance of cellular DNA damage. *Nat. Rev. Mol. Cell Biol.* **13**, 141–152 (2012).
4. M. Vujanovic *et al.*, Replication fork slowing and reversal upon DNA damage require PCNA polyubiquitination and ZRANB3 DNA translocase activity. *Mol. Cell* **67**, 882–890.e5 (2017).
5. B. Pilzecker, O. A. Buoninfante, H. Jacobs, DNA damage tolerance in stem cells, ageing, mutagenesis, disease and cancer therapy. *Nucleic Acids Res.* **47**, 7163–7181 (2019).
6. S. García-Gómez *et al.*, PrimPol, an archaic primase/polymerase operating in human cells. *Mol. Cell* **52**, 541–553 (2013).
7. C. Guo *et al.*, Mouse Rev1 protein interacts with multiple DNA polymerases involved in translesion DNA synthesis. *EMBO J.* **22**, 6621–6630 (2003).
8. J. L. Wojtaszek *et al.*, A small molecule targeting mutagenic translesion synthesis improves chemotherapy. *Cell* **178**, 152–159.e11 (2019).
9. N. Nikolaishvili-Feinberg, M. Cordeiro-Stone, Discrimination between translesion synthesis and template switching during bypass replication of thymine dimers in duplex DNA. *J. Biol. Chem.* **275**, 30943–30950 (2000).
10. C. Yang, D. Tang, PCNA modifications for regulation of post-replication repair pathways. *Comput. Model. Eng. Sci.* **1**, 119–131 (2000).
11. R. Ceccaldi, P. Sarangi, A. D. D'Andrea, The Fanconi anaemia pathway: New players and new functions. *Nat. Rev. Mol. Cell Biol.* **17**, 337–349 (2016).
12. I. Vitale, G. Manic, R. De Maria, G. Kroemer, L. Galluzzi, DNA damage in stem cells. *Mol. Cell* **66**, 306–319 (2017).

13. D. Walter *et al.*, Exit from dormancy provokes DNA-damage-induced attrition in haematopoietic stem cells. *Nature* **520**, 549–552 (2015).
14. A. Wilson *et al.*, Hematopoietic stem cells reversibly switch from dormancy to self-renewal during homeostasis and repair. *Cell* **135**, 1118–1129 (2008).
15. D. Soteriou, Y. Fuchs, A matter of life and death: Stem cell survival in tissue regeneration and tumour formation. *Nat. Rev. Cancer* **18**, 187–201 (2018).
16. B. Pilzecker *et al.*, DNA damage tolerance in hematopoietic stem and progenitor cells in mice. *Proc. Natl. Acad. Sci. U.S.A.* **114**, E6875–E6883 (2017).
17. A. Martín-Pardillos *et al.*, Genomic and functional integrity of the hematopoietic system requires tolerance of oxidative DNA lesions. *Blood* **130**, 1523–1534 (2017).
18. J. M. Prasher *et al.*, Reduced hematopoietic reserves in DNA interstrand crosslink repair-deficient Ercc1-/- mice. *EMBO J.* **24**, 861–871 (2005).
19. B. Schumacher, J. Pothof, J. Vijg, J. H. J. Hoeijmakers, The central role of DNA damage in the ageing process. *Nature* **592**, 695–703 (2021).
20. S. D. Mcculloch, T. A. Kunkel, The fidelity of DNA synthesis by eukaryotic replicative and translesion synthesis polymerases. *Cell Res.* **18**, 148–161 (2008).
21. C. E. Edmunds, L. J. Simpson, J. E. Sale, PCNA ubiquitination and REV1 define temporally distinct mechanisms for controlling translesion synthesis in the avian cell line DT40. *Mol. Cell* **30**, 519–529 (2008).
22. N. Wit *et al.*, Roles of PCNA ubiquitination and TLS polymerases κ and η in the bypass of methyl methanesulfonate-induced DNA damage. *Nucleic Acids Res.* **43**, 282–294 (2015).
23. P. Langerak, A. O. H. Nygren, J. P. Schouten, H. Jacobs, Rapid and quantitative detection of homologous and non-homologous recombination events using three oligonucleotide MLPA. *Nucleic Acids Res.* **33**, e188 (2005).
24. M. J. Muraro *et al.*, A single-cell transcriptome atlas of the human pancreas. *Cell Syst.* **3**, 385–394.e3 (2016).
25. S. J. Morrison, N. Uchida, I. L. Weissman, The biology of hematopoietic stem cells. *Annu. Rev. Cell Dev. Biol.* **11**, 35–71 (1995).
26. D. J. Rossi *et al.*, Deficiencies in DNA damage repair limit the function of haematopoietic stem cells with age. *Nature* **447**, 725–729 (2007).
27. I. M. Ward, J. Chen, Histone H2AX is phosphorylated in an ATR-dependent manner in response to replicational stress. *J. Biol. Chem.* **276**, 47759–47762 (2001).
28. S. Sertic *et al.*, Coordinated activity of Y family TLS polymerases and EXO1 protects non-S phase cells from UV-induced cytotoxic lesions. *Mol. Cell* **70**, 34–47.e4 (2018).
29. T. Ogi *et al.*, Three DNA polymerases, recruited by different mechanisms, carry out NER repair synthesis in human cells. *Mol. Cell* **37**, 714–727 (2010).
30. Y. Xiang *et al.*, RNA m6A methylation regulates the ultraviolet-induced DNA damage response. *Nature* **543**, 573–576 (2017).
31. Y. Yang *et al.*, DNA repair factor RAD18 and DNA polymerase Polκ confer tolerance of oncogenic DNA replication stress. *J. Cell Biol.* **216**, 3097–3115 (2017).
32. L. J. Norton *et al.*, KLF1 directly activates expression of the novel fetal globin repressor ZBTB7A/LRF in erythroid cells. *Blood Adv.* **1**, 685–692 (2017).
33. T. Maeda *et al.*, LRF is an essential downstream target of GATA1 in erythroid development and regulates BIM-dependent apoptosis. *Dev. Cell* **17**, 527–540 (2009).
34. J. Borg *et al.*, Haploinsufficiency for the erythroid transcription factor KLF1 causes hereditary persistence of fetal hemoglobin. *Nat. Genet.* **42**, 801–807 (2010).
35. E. M. Pietras *et al.*, Functionally distinct subsets of lineage-biased multipotent progenitors control blood production in normal and regenerative conditions. *Cell Stem Cell* **17**, 35–46 (2015).
36. T. W. Braun, M. K. Kuoch, E. Khandros, H. Li, FACS and immunomagnetic isolation of early erythroid progenitor cells from mouse fetal liver. *STAR Protoc.* **3**, 101070 (2022).
37. F. Soares-Da-Silva *et al.*, Yolk sac, but not hematopoietic stem cell–derived progenitors, sustain erythropoiesis throughout murine embryonic life. *J. Exp. Med.* **218**, e20201729 (2021).
38. A. Planutis *et al.*, Neomorphic effects of the neonatal anemia (Nan-Eklf) mutation contribute to deficits throughout development. *Development* **144**, 430–440 (2017).
39. M. Siatecka *et al.*, Severe anemia in the nan mutant mouse caused by sequence-selective disruption of erythroid Krüppel-like factor. *Proc. Natl. Acad. Sci. U.S.A.* **107**, 15151–15156 (2010).
40. L. Perié, K. R. Duffy, L. Kok, R. J. De Boer, T. N. Schumacher, The branching point in erythro-myeloid differentiation. *Cell* **163**, 1655–1662 (2015).
41. J. I. Garaycoechea *et al.*, Alcohol and endogenous aldehydes damage chromosomes and mutate stem cells. *Nature* **553**, 171–177 (2018).
42. K. Busch *et al.*, Fundamental properties of unperturbed haematopoiesis from stem cells in vivo. *Nature* **518**, 542–546 (2015).
43. A. Spanjaard *et al.*, Division of labor within the DNA damage tolerance system reveals non-epistatic and clinically actionable targets for precision cancer medicine. *Nucleic Acids Res.* **50**, 7420–7435 (2022).
44. A. Lunardi, J. Guarnerio, G. Wang, T. Maeda, P. P. Pandolfi, Role of LRF/Pokemon in lineage fate decisions. *Blood* **121**, 2845–2853 (2013).